Visualization of pore water colloids in intact soil using a new Diffusive Gradients in Thin Films (DGT)-based approach

Claudia Moens[1,*], Justin Payne[2], Casey L. Doolette[2], Camille Resseguier[5], Jan Vanderborght[1,4], Enzo Lombi[3], Erik Smolders[1]

[1]Division of Soil and Water Management, KU Leuven, Kasteelpark Arenberg 20, 3001 Heverlee, Belgium

[2]Adelaide University, Mawson Lakes, South Australia 5095, Australia

[3]Future Industries Institute, Adelaide University, Mawson Lakes, South Australia 5095, Australia.

[4] Agrosphere Institute, IBG-3, Forschungszentrum Jülich, Germany

[5]Université Paris-Saclay, INRAE, AgroParisTech, UMR EcoSys, 91120 Palaiseau, France

[*]Corresponding Author

Claudia Moens (claudia.moens@kuleuven.be), Erik Smolders (erik.smolders@kuleuven.be), Justin Payne (justin.payne@adelaide.edu.au), Casey L. Doolette (casey.doolette@adelaide.edu.au), Camille Resseguier (Camille.Resseguier@inrae.fr), Jan Vanderborght (j.vanderborght@fz-juelich.de), Enzo Lombi (e.lombi@adelaide.edu.au)
[*]Corresponding Author

Supporting information

S1 Climatologic data of the sampling site

The cumulative precipitation in the weeks preceding and surrounding sampling, from December 1 2023 till February 28 2024 was 233 mm, this is close to the 90th percentile (230.4 mm) of cumulative precipitation for these months since 1950, measured in Trappes.

February 2024 was also warm, the monthly average of daily maximum temperatures was 10.9 °C, which is higher than the 90th percentile value for February since 1950, the monthly average of daily minimum temperatures is 6.3 °C in February 2024, which is the highest measured value since 1950. Data are freely available at Meteo France (Accueil | meteo.data.gouv.fr).

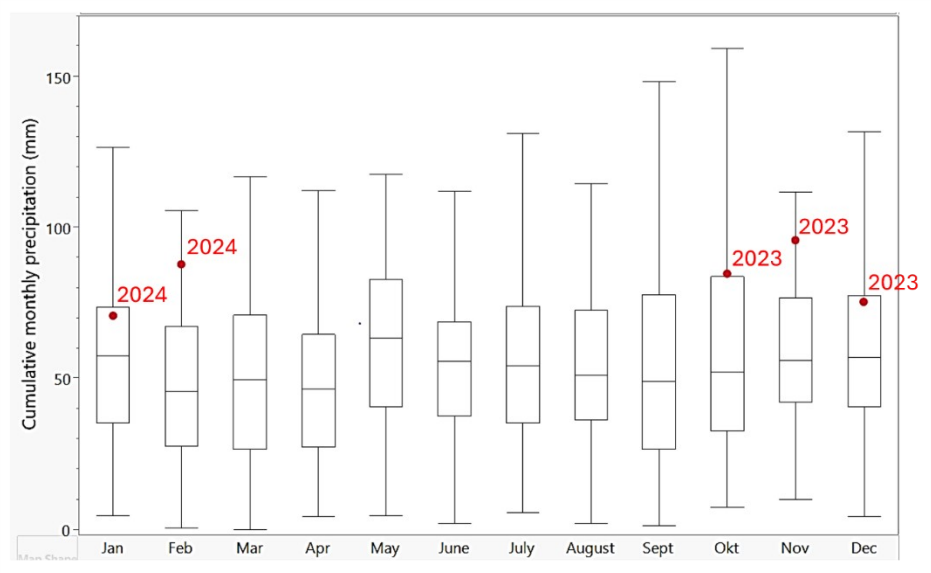

Figure S1 Boxplots showing the cumulative monthly precipitation in a nearby weather station. The dots indicate the rainfall in the months preceding sampling in February 2024.

S2 Binding layer imaging with X-ray Fluorescence Microscopy

The X-ray fluorescence mapping of Fe and Mn was performed at the XFM beamline of the Australian Synchrotron (ANSTO) in Melbourne, Victoria. Samples were analyzed at the microprobe end-station with the MAIA detector. The binding layers were mounted on Perspex sample mounts using double-sided tape. The scanned area is approximately 10 cm x 5 cm, starting at the top of the BL. The samples were scanned with the horizontal axis in continuous motion with spot size of 10 µm and scan speed of 10 mm/s with discrete vertical steps that matched the resolution in the *x*-direction (120 µm). The transit time per pixel was set to 12 ms, which allows fast detection of Fe and Mn on the binding gels. The photon energy of the incident X-ray beam was set at 10.0 keV using a Si(111) monochromator. The Mn and Fe data were processed using GeoPIXE and maps were exported to ImageJ.

S3 Field Flow Fractionation analysis

Briefly, the carrier solution is 1 mM NH_4HCO_3 at pH 8.3, the membrane is 1 kDa polyether sulfone, the spacer thickness is 500 μm. Pore waters were measured undiluted and the injected sample volume was 1 mL. A gradient in cross-flow was applied in the elution phase to separate a broad size distribution of colloids, starting with a constant cross-flow of 1.5 mL min^{-1} for 30 min to separate small particles (< 30 nm, based on FlFFF theory) with high resolution, followed by a linear decrease to 0.2 mL min^{-1} in two minutes, which was kept constant for another 30 minutes to separate particles up to 100 nm (previously determined with polystyrene standards of 100 nm). Next, the cross-flow was set to 0 mL min^{-1} for another 20 min. Particles that elute at zero cross-flow are not further size-separated as described by Neubauer et al. (2013), nevertheless, they have a size between 100 and 450 nm (and residual particles of any size that were previously sorbed on the PES membrane and released when the cross-flow is stopped).

S4 Clay mineralogy characterization in soil

Clay separation was done with a modified Jackson treatment (Jackson, 1975) according to Zeelmaekers (2011). First, carbonates were dissolved using sodium acetate at pH 5 in a water bath at 90°C; second, organic material and MnO_2 were oxidised and removed with 7% H_2O_2 in a water bath at 60°C; third, Fe and Al oxyhydroxides were removed with a citrate-bicarbonate-dithionite solution in a water bath at 80°C. The remaining fraction was size-separated < 0.2 µm and < 2 µm by centrifugation. A subset of the < 0.2 µm fraction of MSW soil was dialysed (VISKING®, MWCO 12 kDa to 14 kDa) in mQ water that was replaced several times during one week to remove excess salt, that fraction was used in the DGT performance test. For the remaining fractions (< 0.2 µm and < 2 µm of MSW and FYM), the interlayers were saturated by calcium ions and flocculated with 1 M $CaCl_2$, dialysed in demi water as described before to remove excess salts and applied on a glass slide for XRD analysis. Data processing was done using Profex software. Each of the four fractions were also analysed after digestion with the $LiBO_4$ fusion method in graphite crucibles (Suhr, N.H. & Ingamells, C.O. 1966) to break down the silicate structure. The elemental composition of the clays was measured with ICP-MS (Agilent 7700).

S5 Analysis of clay on the BL with acid digestion

Preliminary tests showed that colloids could not be quantitatively eluted from hydrogels using standard elution procedures, possibly indicating that colloids are retained in the hydrogel pores and/or colloids were not stable in the eluate. Therefore, the methodology to analyse clay colloids on the binding gels was on destructive analysis of the binding layer and clay colloids. Three different digestion procedures were tested in their ability to quantitatively analyze Al, Si, Fe from clay colloids adsorbed on DGT binding layers. The aim was to find a methodology to analyse Si, Al and Fe as the stoichiometry helps to identify clay colloids (from Si/Al ~ 2) from Al and Fe oxyhydroxides in environmental samples.

Clay elemental analysis is typically done with HF digestion, as this acid is crucial for breaking down the aluminosilicate structure. The HF digestion method also completely dissolves the ZrO_2 BL. However, the method yielded too high LOQ measured on gel blanks to detect clay on the samples from the performance test (see below), therefore 2 alternative digestion methods were tested; Aqua Regia (open block) and high-temperature microwave digestion (210°C) with H_2SO_4, HCl and HNO_3 acids.

- HF digestion: The isolated clay powders (10 mg) and dried BL gels (circles of 3.14 cm^2, thickness 400 µm) are digested overnight at room temperature in 15 mL polypropylene tubes with a combination of HF (0.5 mL) + HNO_3 (0.3 mL). Next, HCl 1 mL is added to stabilize Fe and Al in solution and samples are heated with sample tubes closed to avoid loss of volatile SiF_4 in a water bath at 80°C for 6 hours. The HF is subsequently neutralized using 5 mL H_3BO_3 (4% w/v) in a water bath at 80°C for 6 hours. The gel samples are diluted additionally 10 times with mQ water to reduce the B levels to 230 mg/L B for ICP-MS analysis. Clay samples were diluted additionally 1000 times.
- Aqua Regia digestion: The isolated clay powders (10 mg) and dried gels are digested with 2 mL Aqua Regia (HCl:HNO_3 3:1) in an open block for 4 hours at 90°C and evaporated until nearly dry at 120°C. The samples are diluted to 10 mL using mQ water. The clay samples are

additionally diluted 1000 times. The Zr-containing binding layers are not completely dissolved with this procedure, as Zr oxides do not dissolve in aqua regia. The advantage of the method is the low sample dilution (1 gel in 10 mL).

- High-temperature H_2SO_4/HNO_3/HCl digestion: The isolated clay powders (10 mg) and dried gels are digested in a mixture of HNO_3 (2 mL) and H_2SO_4 (4 mL) in closed Teflon vessels at high temperature (210°C) using MARS6 microwave. The H2SO4 lowers boiling temperature and therefore allows temperatures up to 210 °C, while the HNO_3 absorbs microwaves. Fist a predigest is done for 30 minutes at 180°vessels are allowed to cool down and a second digestion run is done at 210°C for 30 minutes. Finally, to the sample is added 0.5 mL HCl to stabilize Fe and Al. The samples are diluted to 50 mL in the vessels and additionally diluted 1:2 with mQ water to dilute to reduce the viscosity of the H2SO4 and reduce the acidity to acceptable levels for ICP-MS detection. The clays are diluted additionally 1000 times. The Zr-containing binding layers are completely dissolved with this procedure, but the disadvantage is the 10 times higher dilution (1 gel in 100 mL) compared to the Aqua Regia digestion.

First, digestion procedures were verified for their ability to quantitatively analyse Al, Si and Fe in the powdered clay sample (with reference to $LiBO_3$ values) and the limit of quantification (LOQ) was measured on 3 gel blanks. Next, analysis of clay was done with or without the presence of a BL. The samples consist of 300 µL clay suspensions at various dilutions that are spiked in digestion tubes with or without binding layer (discs of 3.14 cm^2, same BL as in the experiment).

The samples are spiked with internal standard and analysis with ICP-MS is done with direct injection in the nebulizer, not using sample introduction system with 6-way valve, because of strong carry-over (due to high B concentrations in HF method and high Zr concentrations in HF and H_2SO_4 method).

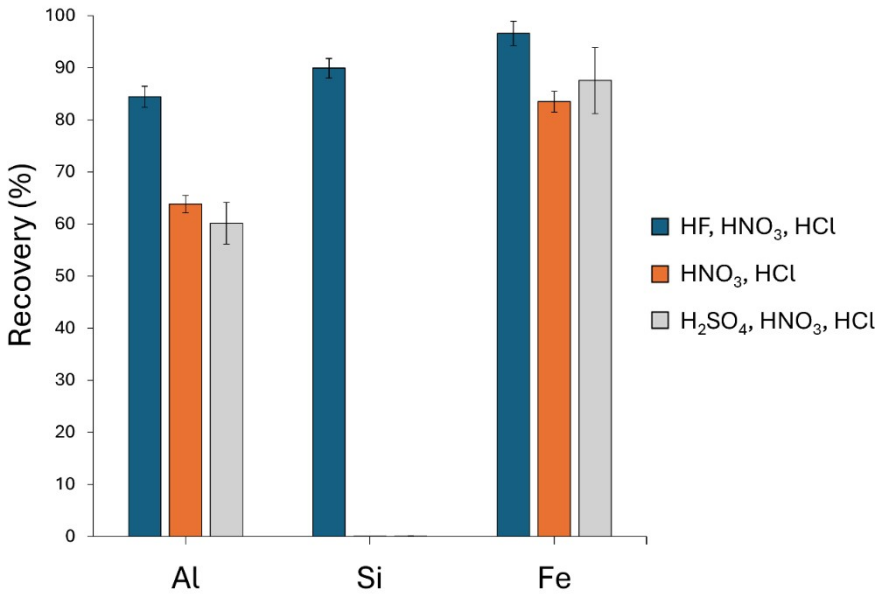

Figure S2 Recovery of Al, Si, Fe in isolated clay samples measured with 3 different digestion procedures. The recovery was calculated with reference to the clay analysis with lithium metaborate fusion and indicates that the HF method was the only method that allowed for quantitative analysis of Si, Al, Fe in clay with high recovery. The Aqua Regia method and the high-temperature H2SO4 method did not dissolve the silicates as part of the clay structure with very low Si recovery (< 1%) and low Al recovery (<65%). The Fe recovery was high for all methods (> 84%).

Table S1 Limit of Quantification (LOQ) calculated from the average + 3 SD (Standard Deviation) of the concentration measured in 3 blank gels.

	Al	Si	Fe
Digestion method	*µmol/cm²*	*µmol/cm²*	*µmol/cm²*
Aqua Regia	0.088		0.005
High-T H_2SO_4	0.005		0.007
HF	0.210	0.636	0.030

The expected minimal concentrations of Al, Si, Fe on the hydrogels of the performance test are calculated based on the hydrogel volume and the test suspension concentrations (see below).

Table S2 Expected minimal concentration of Al, Si, Fe for DET hydrogels in equilibrium with colloid the suspension concentrations.

	Al	Si	Fe
Suspension	*µmol/cm²*	*µmol/cm²*	*µmol/cm²*
Isolated Clay	0.003	0.006	0.001
Soil Extract	0.050	0.094	0.017

The HF method was the only method that allowed quantitative recovery of Al and Si in clay. However, from the gel blank analysis appeared that the LOQ of Si and Al is too high to detect these elements on the hydrogels from the performance test. In subsequent tests, the focus of clay colloid detection was therefore based on Fe. The digestion methods were tested which one can analyse Fe with high recovery at a range of clay concentrations including those expected of the performance test. From that test the High-Temperature H_2SO_4 method was selected as best performing because the recovery + gel was generally higher than the AR method and the AR digestion does not completely digest the Zr oxide based BL. The detection limits of the high-T method are lower for Fe compared to the HF method and allowed to quantitatively analyse Fe also in presence of the binding layer. This method is therefore used in subsequent analysis to determine colloid binding based on Fe. Nevertheles, the samples of isolated clay suspension were still below LOQ for this method.

Table S3 Recovery of Fe (average + SD with dublicate samples) with and without gel for range in colloid concentrations measured after different digestion procedures.

Nominal Fe	AR	AR (+ gel)	µwave	µwave (+ gel)	HF	HF (+ gel)
µmol/cm²	*%*	*%*	*%*	*%*	*%*	*%*
0.0017	< DL	< DL	< DL	< DL	< DL	< DL
0.0168	98±<1	101±2	66±2	79±4	< DL	< DL
0.1684	96±1	84±5			91±2	91±<1
1.6842	97±<1	60±3	87±4	92±2	94±1	94±3

S6 Settings LA-ICP-MS setup used in the performance test

The LA-ICP-MS analysis of the BL was performed in line scan mode. Horizontal lines of 30 mm were ablated on the BL with interline distance of 120 µm and 40 lines per gel (10 for blank gels). The laser beam was 80 µm squared, the repetition rate was 20 Hz and scan speed was 400 µm s^{-1}.

The ICP-MS monitored the elements ^{12}C (5 ms), ^{27}Al (25 ms), ^{28}Si (50 ms), ^{31}P (25 ms), ^{56}Fe (25 ms), ^{85}Rb (25 ms), ^{90}Zr (5 ms), ^{133}Cs (25 ms), dwell time between brackets (total cycle time 200 ms), in MS/MS mode, all elements on mass. The method used H_2 in the cell gas at 2 mL min^{-1} to reduce the polyatomic interferences on Si. Preliminary method development on reference sample NIST610 indicated low signal to noise ratio for Si without the use of reaction gas (No Gas Mode) or with He gas at 10 mL min^{-1} (HEHe mode). The H_2 gas did not reduce the sensitivity importantly of the other elements.

S7 Results Flow Field Flow Fractionation analysis

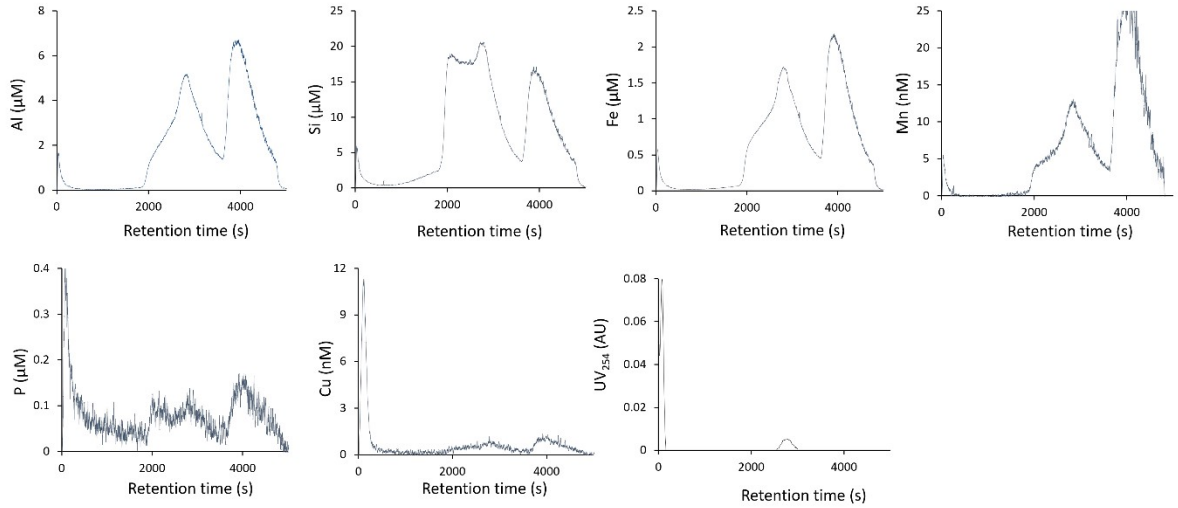

Figure S3 Flow Field Flow Fractionation fractograms from the pore water of MSW soil.

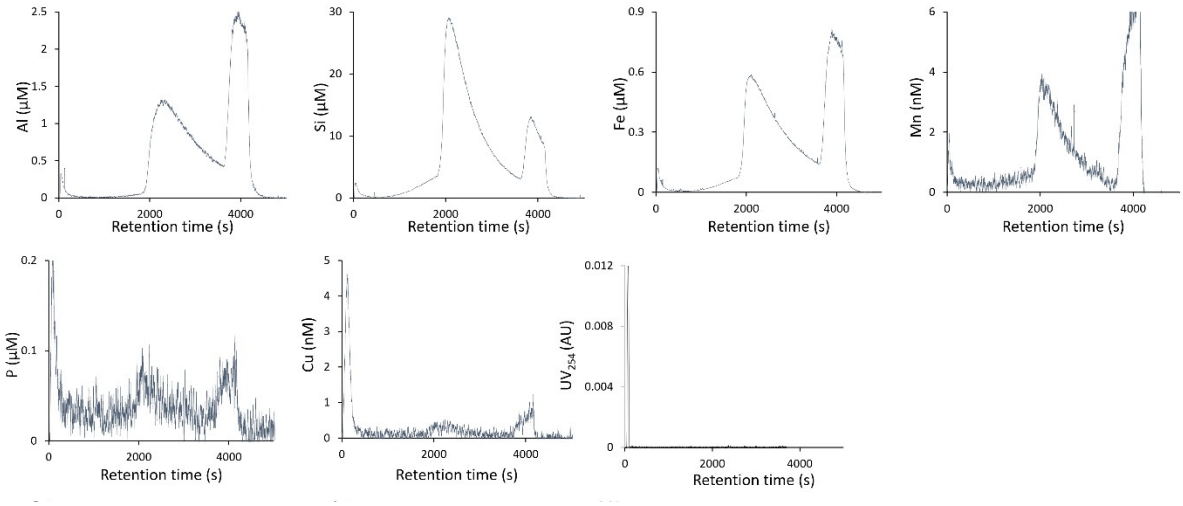

Figure S4 Flow Field Flow Fractionation fractograms from the pore water of the control treatment (CON).

Table S4 The FlFFF fractograms were divided into organic (T_r 0-5 min) and mineral (T_r 5- 82 min) colloid fractions, and colloidal concentrations were calculated by integration. These concentrations were expressed as fractions of the total pore water concentrations. Truly dissolved ions (TD) (< 1 kDa) are not measured with FlFFF analysis, their concentrations in pore water were estimated as the fraction of the total pore water concentration not recovered by FlFFF.

FYM soil:

	Pore water concentration (µM)	TD (%)	Organic (%)	Mineral (%)
P	41	77	3.3	19
Al	284	15	0.9	84
Fe	104	21	0.8	79
Mn	1.1	37	1.1	62
Si	1394	47	0.5	53

MSW soil:

	Pore water concentration (µM)	TD (%)	Organic (%)	Mineral (%)
P	6.2	10	19	70
Al	157	0.1	1.8	101
Fe	56	4	1.7	94
Mn	0.7	21	1.2	78
Si	1119	42	1.0	57

CON soil:

	Pore water concentration (µM)	TD (%)	Organic (%)	Mineral (%)
P	5.1	37	9.7	53
Al	61	27	1.1	72
Fe	23	28	1.0	71
Mn	0.3	65	1.3	34
Si	1024	51	0.5	49

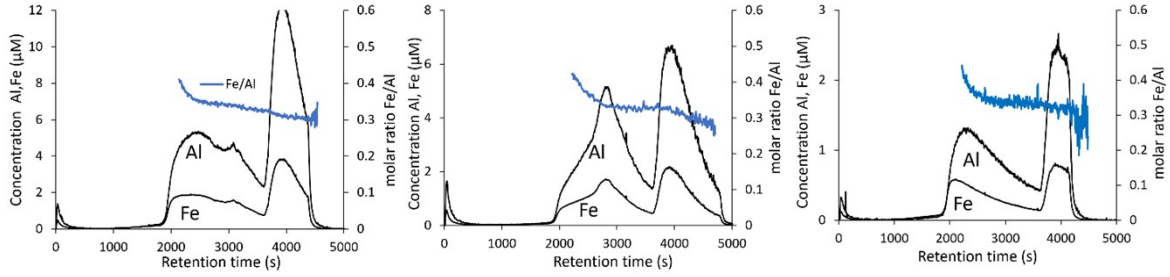

Figure S5 The colloid composition is derived from FlFFF fractograms by calculating at each time point molar Fe/Al element ratios, and the median molar ratio over the relevant mineral colloid size range is taken. This analysis shows a similar composition (molar Fe/Al ratio) in pore water colloids from the three soil treatments (left: FYM, middle: MSW and right: CON), the molar Fe/Al ratio in the mineral colloids is on average 0.33 over the full size distribution.

S8 Clay composition and mineralogy in soil

The clay fraction (< 2 µm & < 0.2 µm) was separated by Jackson treatment followed by X-ray diffraction measurements (XRD). Clay mineralogy was determined by measurement of basal spacing parameters on the clay fraction in oriented in glass slides: 2 to 50 °2θ range, 2° 2θ step size. The samples were measured air dried and ethylene glycol solvated. Identification of clay minerals was done using Sybilla software and based on the d-spacing value of their 00/ (mainly 001) reflections.

The XRD analysis on clay fraction (<2 µm and <0.2 µm) sampled in the plough pan of FYM and MSW indicates that the clay primarily consists of the 2:1 clay types illite, smectite, mixed layer illite-smectite and with the 1:1 type clay kaolinite. This is in agreement with the clay mineralogy characterisation in the LUCAS database (Panagos et al. 2022). In 2 sampling points within 100 km from the field trial, the clay mineralogy in topsoil is described as dominantly illite, mixed layer illite-smectite, with kaolinite. The nanoparticulate clay fraction (< 0.2 µm) is in terms of mineralogy and composition very similar to the < 2 µm fraction and similar for both soils (MSW and FYM).

Illite (2:1)

Illite was identified using Sybilla software. In addition, the XRD pattern after glycolation showed that the 001 and 002 reflections at 10 and 5 Å did not change upon glycolation. Glauconite has similar XRD pattern than illite, but does not form naturally in the submicron range (< 0.2 µm) as a dominant particle size.

Smectite (2:1)

Smectite (S) was identified based on Air-dried peak at 14 Å that expands to 17 Å with ethylene glycol. Distinction of the different mineral species within the smectite group (e.g. Montmorilonite, nontronite) would be possible only after additional treatments and XRD measurements (Panagos et al., 2022).

Mixed-layer Illite/smectite (I/S) was identified based on a broad reflection between 10 and 14 Å, which changes upon glycolation, forming a very broad, diffuse reflection at higher d-spacing values

than smectite. When it is present in higher amount, it can be also identified by its broad 002 reflection between 8.5 –10Å, which is not the case here (Panagos et al., 2022).

Vermiculite is present when a sharper peak around 14.3 Å, which does not shift upon glycolation, or showed just a small expansion, which is not the case here. However, conventionally vermiculite identification requires additional treatments and XRD measurements by checking if it collapses under K-exchange at ambient T to 10 Å (Panagos et al., 2022). The use of ethylene glycol is strictly not able to accurately differentiate between smectite and vermiculite.

Kaolinite (1:1)

Kaolinite was identified using Sybilla software. The reflection at 12.6 Å that does not change after glycolation could also indicate chlorite (2:1:1 type clay), but chlorite was not identified by Sybilla software (i.e. absence of 4.7 Å peak).

Table S5 Clay composition analysis on the clay fraction < 0.2 µm and < 2 µm obtained from the plough pan of soil after Jackson treatment (see main text). The average and standard deviation is given for MSW and FYM soil combined. The molar Si/Al ratio in the clay colloids (< 0.2 µm) is 1.86, the molar Fe/Al ratio in the clay colloids is 0.24.

	< 0.2 µm		< 2 µm	
	wt%	µmol/g	wt%	µmol/g
Si	21.4 ± 0.3	7610 ± 67	22.6 ± 0.1	8051 ± 8
Al	11.5 ± 0.1	4268 ± 34	11.7 ± 0.1	4336 ± 6
Fe	5.7 ± 0.1	1015 ± 12	4.8 ± 0.1	852 ± 10
K	2.1 ± <0.1	530 ± 6	2.7 ± <0.1	681 ± 4
Ca	1.3 ± <0.1	335 ± 6	1.1 ± 0.1	285 ± 33
Mg	1.3 ± <0.1	517 ± 9	1.2 ± <0.1	501 ± 8
P	0.05 ± 0.01	15 ± 2	0.04 ± <0.01	13 ± <0.1

S9 X-ray fluorescence microscopy (XFM) and Laser-Ablation (LA)-ICP-MS analysis of DGT BL

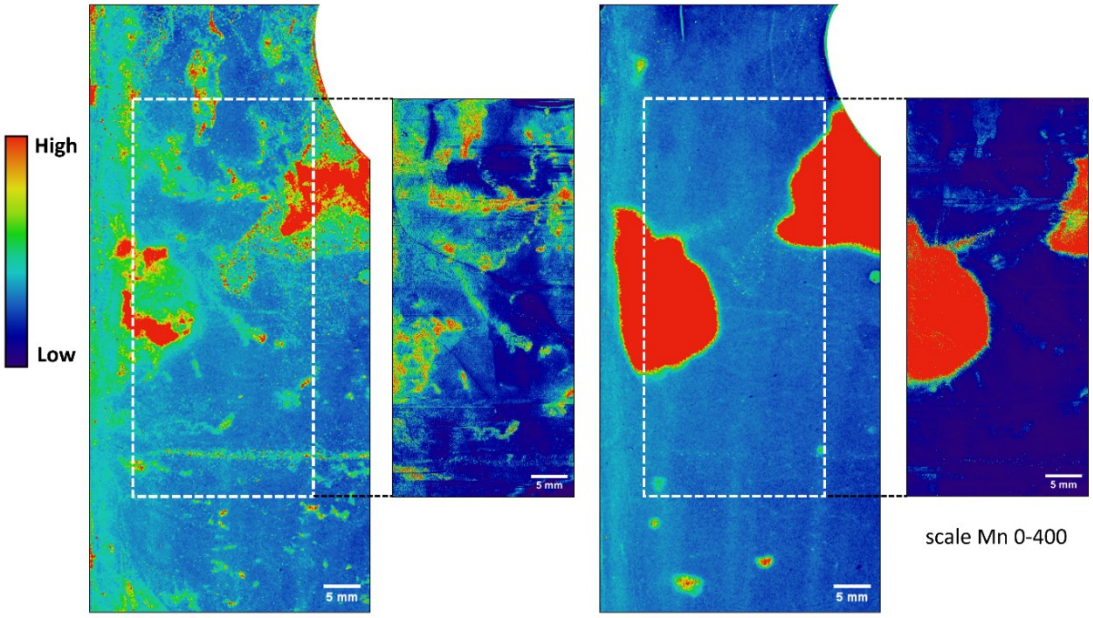

Figure S6 Elemental maps of Fe (left) and Mn (right) obtained with XFM, the inset shows the smaller area measured with LA-ICP-MS for FYM soil. The colour scale indicates low to high intensity values, and is the same in Figure S6 and S7 for Fe, but the highest intensity values for Mn differs (i.e. here up to 400).

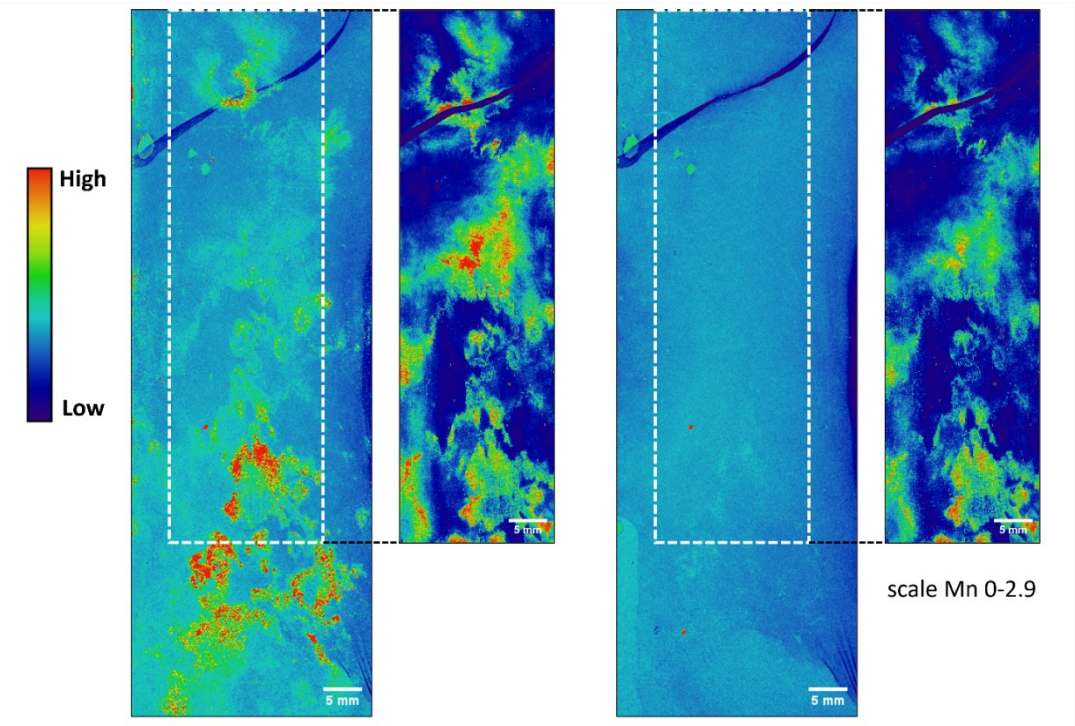

Figure S7 Elemental maps of Fe (left) and Mn (right) obtained with XFM, the inset shows the smaller area measured with LA-ICP-MS for MSW soil (replicate 2). The colour scale indicates low to high intensity values, and is the same in Figure S6 and S7 for Fe, but the highest intensity values for Mn differs (i.e. here up to 2.9).

S10 LA-ICP-MS maps and statistical analysis for all samples on whole images

MSW

Table S6 Skewness of pixel intensity values before and after log_{10} transformation. The number of pixels is 225225.

	Untransformed	log_{10}
Al	2.61	0.16
Si	3.21	0.25
Fe	2.43	0.18
Ca	127.55	0.18
Mg	2.96	0.26
K	3.70	0.31
Rb	3.31	0.43
Cs	3.15	0.33
Mn	3.62	0.23
P	4.16	-0.54

Table S7 Pixel-wise correlation coefficients on log_{10} transformed data for MSW soil

	$Log_{10}Al$	$Log_{10}Si$	$Log_{10}Fe$	$Log_{10}Mn$	$Log_{10}Ca$	$Log_{10}Mg$	$Log_{10}K$	$Log_{10}P$	$Log_{10}Rb$	$Log_{10}Cs$
$Log_{10}Al$	1									
$Log_{10}Si$	0.98	1								
$Log_{10}Fe$	1.00	0.98	1							
$Log_{10}Mn$	0.98	0.96	0.98	1						
$Log_{10}Ca$	0.60	0.62	0.60	0.58	1					
$Log_{10}Mg$	0.99	0.98	0.99	0.97	0.64	1				
$Log_{10}K$	0.98	0.98	0.98	0.97	0.61	0.98	1			
$Log_{10}P$	0.49	0.50	0.49	0.47	0.80	0.51	0.50	1		
$Log_{10}Rb$	0.98	0.97	0.98	0.96	0.59	0.97	0.98	0.46	1	
$Log_{10}Cs$	0.94	0.94	0.94	0.93	0.56	0.94	0.94	0.44	0.94	1

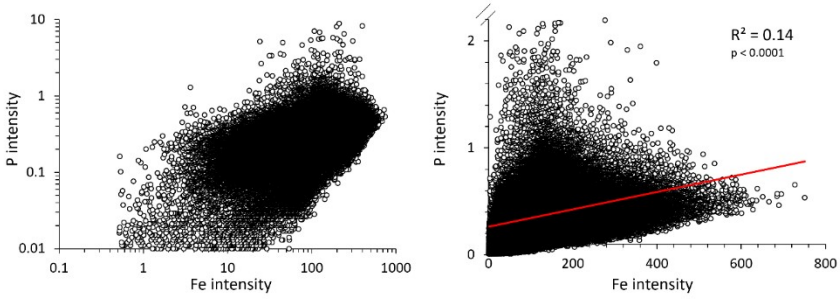

Figure S8 There is no strong linear relationship between P and Fe on the binding layer. The correlation coefficient between Fe and P is not strong (r = 0.49), which indicates that colloidal Fe does not make an important contribution to mobile P (left panel), data for MSW soil. With increasing Fe, also P increases, but the highest P occurred in regions where Fe concentrations were relatively low, which is in line with truly dissolved and organic P measured in the pore water analysis and low P binding on the colloids.

FYM

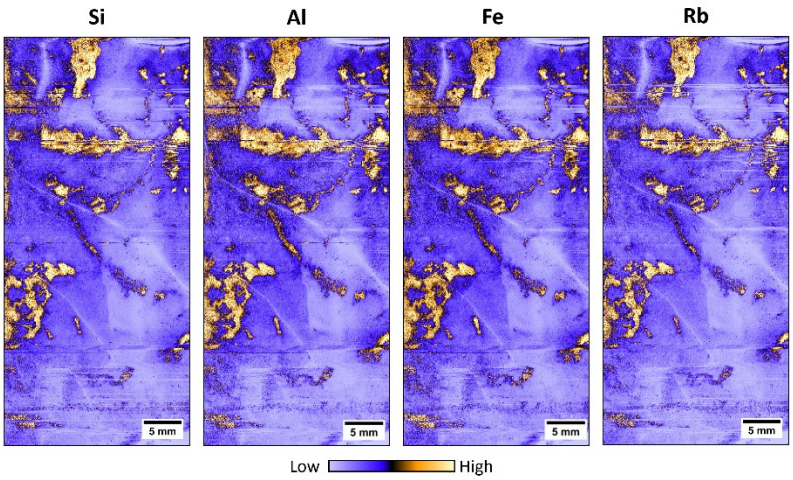

Figure S9 Selection of elemental maps for MSW soil obtained with LA-ICP-MS analysis.

Table S8 Skewness of pixel intensity values before and after log_{10} transformation. The number of pixels is 276914.

	Untransformed	log_{10}
Al	1.457	-0.650
Si	2.166	-0.451
Fe	1.397	-0.683
Ca	3.855	-0.710
Mg	2.073	-0.302
K	2.948	-0.265
Rb	2.462	-0.085
Cs	2.239	-0.175
Mn	6.489	0.884
P	5.286	-1.364

Table S9 Pixel-wise correlation coefficients on log_{10} transformed data for FYM soil

	$Log_{10}Al$	$Log_{10}Si$	$Log_{10}Fe$	$Log_{10}Mn$	$Log_{10}Ca$	$Log_{10}Mg$	$Log_{10}K$	$Log_{10}P$	$Log_{10}Rb$	$Log_{10}Cs$
$Log_{10}Al$	1									
$Log_{10}Si$	0.97	1								
$Log_{10}Fe$	0.99	0.98	1							
$Log_{10}Mn$	0.66	0.66	0.67	1						
$Log_{10}Ca$	0.64	0.61	0.62	0.70	1					
$Log_{10}Mg$	0.99	0.98	0.98	0.68	0.66	1				
$Log_{10}K$	0.96	0.98	0.97	0.63	0.56	0.96	1			
$Log_{10}P$	0.48	0.53	0.52	0.61	0.76	0.51	0.50	1		
$Log_{10}Rb$	0.96	0.98	0.97	0.63	0.58	0.97	0.98	0.47	1	
$Log_{10}Cs$	0.94	0.95	0.94	0.61	0.56	0.94	0.94	0.45	0.95	1

Sample CON

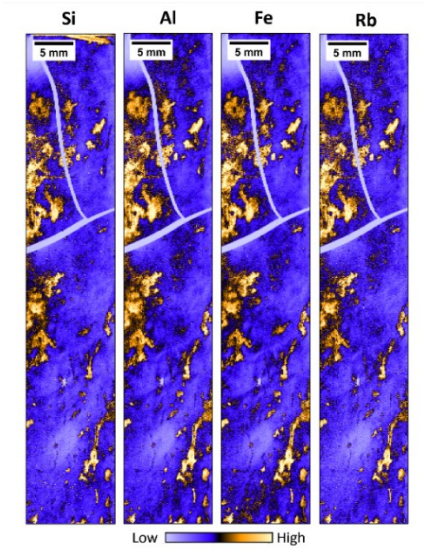

Figure S10 Selection of elemental maps for CON soil obtained with LA-ICP-MS analysis. The size of the image is 11 x 63 mm.

Table S10 Skewness of pixel intensity values before and after log_{10} transformation. The number of pixels is 144005.

	untransformed	log_{10}
Al	1.660	-1.778
Si	2.020	-1.045
Fe	1.709	-2.110
Ca	50.096	1.790
Mg	2.867	-1.370
K	8.721	-0.962
Rb	2.381	-0.050
Cs	1.935	-0.193
Mn	14.477	-1.014
P	17.626	-1.528

Table S11 Pixel-wise correlation coefficients on log_{10} transformed data for CON soil

	$Log_{10}Al$	$Log_{10}Si$	$Log_{10}Fe$	$Log_{10}Mn$	$Log_{10}Ca$	$Log_{10}Mg$	$Log_{10}K$	$Log_{10}P$	$Log_{10}Rb$	$Log_{10}Cs$
$Log_{10}Al$	1									
$Log_{10}Si$	0.95	1								
$Log_{10}Fe$	0.98	0.94	1							
$Log_{10}Mn$	0.92	0.88	0.94	1						
$Log_{10}Ca$	0.25	0.24	0.21	0.31	1					
$Log_{10}Mg$	0.99	0.94	0.97	0.92	0.32	1				
$Log_{10}K$	0.96	0.95	0.93	0.89	0.28	0.95	1			
$Log_{10}P$	0.16	0.14	0.19	0.23	0.39	0.17	0.15	1		
$Log_{10}Rb$	0.95	0.91	0.92	0.87	0.28	0.95	0.94	0.16	1	
$Log_{10}Cs$	0.88	0.85	0.86	0.81	0.24	0.87	0.86	0.15	0.87	1

S11 Hotspot analysis on LA-ICP-MS maps for all samples

Table S12: Fractional overlap of elemental hotspots, indicating co-localization within high-intensity zones. The table is read row-wise; for example, in MSW soil, 0.93 of Fe hotspots overlap with Al hotspots, whereas 0.99 of Al hotspots overlap with Fe hotspots. The color shading denotes high (red) to low (green) overlap.

MSW soil

	Fe	Al	Si	Rb	Cs	Mn	P	Ca
Fe		0.93	0.84	0.83	0.84	0.84	0.29	0.60
Al	0.99		0.88	0.88	0.88	0.88	0.30	0.63
Si	0.99	0.97		0.95	0.94	0.92	0.29	0.64
Rb	0.98	0.97	0.95		0.94	0.92	0.30	0.64
Cs	0.98	0.96	0.92	0.93		0.91	0.29	0.63
Mn	0.97	0.95	0.90	0.90	0.90		0.27	0.61
P	0.18	0.17	0.15	0.15	0.15	0.14		0.68
Ca	0.41	0.39	0.37	0.37	0.37	0.36	0.63	

FYM soil

	Fe	Al	Si	Rb	Cs	Mn	P	Ca
Fe		0.92	0.83	0.79	0.77	0.04	0.15	0.22
Al	0.89		0.84	0.82	0.79	0.04	0.16	0.24
Si	0.86	0.89		0.92	0.88	0.04	0.15	0.24
Rb	0.81	0.87	0.92		0.89	0.04	0.15	0.25
Cs	0.80	0.85	0.88	0.89		0.16	0.14	0.25
Mn	0.04	0.05	0.05	0.05	0.07		0.50	0.65
P	0.08	0.08	0.08	0.08	0.07	0.22		0.59
Ca	0.12	0.14	0.13	0.14	0.13	0.63	0.58	

CON soil

	Fe	Al	Si	Rb	Cs	Mn	P	Ca
Fe		0.91	0.80	0.82	0.78	0.75	0.15	0.34
Al	0.88		0.81	0.86	0.80	0.71	0.12	0.33
Si	0.74	0.77			0.70	0.64	0.14	0.34
Rb	0.83	0.90			0.81	0.72	0.14	0.34
Cs	0.80	0.84	0.77	0.81		0.68	0.14	0.32
Mn	0.87	0.85	0.80	0.82	0.77		0.20	0.42
P	0.06	0.05	0.07	0.06	0.06	0.08		0.27
Ca	0.11	0.11	0.14	0.12	0.11	0.17	0.28	

Table S13 Pixel-wise Pearson correlation coefficients (r) between P and Fe and Fe/Si calculated in the Fe hotspots only. The pixel intensity values were log_{10}-transformed.

		r	p-value
MSW	Fe	0.08	<0.0001
	Fe/Si	0.13	<0.0001
FYM	Fe	0.17	<0.0001
	Fe/Si	0.03	<0.0001
CON	Fe	0.23	<0.0001
	Fe/Si	0.14	<0.0001

S12 Performance of the DGT method to sample clay colloids from suspension

Table S14 Concentration of a selection of elements in the isolated clay suspension and the soil extract measured at the start of the experiment (Initial) and after 48h deployment (End). The dialysis sample (< 1 kDa) is used to verify truly dissolved concentrations.

<DL: below detection limit

	Al µM	Si µM	P µm	Fe µM	Rb µM	Cs µM
Isolated Clay						
Initial	20	34	<DL	5.1	0.012	0.0005
End	20	35	<DL	5.1	0.012	0.0005
Dialysis	0.1	1.0	<DL	0.2	< DL	< DL
Soil extract						
Initial	294	555	4.9	102	0.190	0.0074
End	284	523	4.8	101	0.182	0.0072
Dialysis	1.9	19	0.3	0.6	< DL	< DL

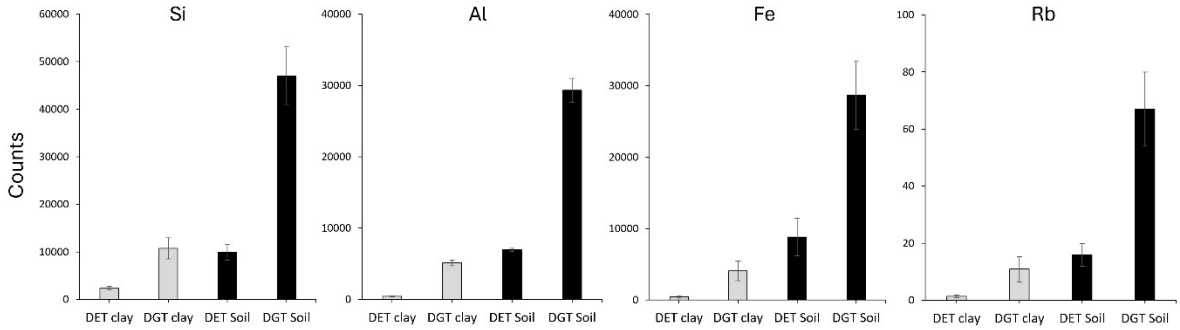

Figure S11 The average Si, Al, Fe and Rb signal (counts, gas blank subtracted) measured in dried hydrogels with LA-ICP-MS. The gels were deployed in suspensions of isolated clay (referred to as "clay") or soil colloids in a $CaCl_2$ extract (referred to as "Soil"), more information in the main text. The Al, Si, Fe and Rb signal in the hydrogels (referred to as "DET") is significantly lower than in the hydrogels with ZrO_2-Chelex (referred to as DGT), which suggests that the BL accumulated clay colloids compared to suspension concentrations. The error bars are standard deviations of the average Al signal per ablated line scan.

Part of the DGT BL measured concentrations might be truly dissolved ions, not colloids, because ions diffuse faster than colloids and because the Al and Fe ions also bind to the Chelex (Panther et al. 2012) and Si to ZrO_2 (Guan et al. 2024) in the binding layer. An estimate of the contribution of truly dissolved ions on the BL concentrations is calculated below.

First, the elemental concentration on the BL is calculated from the DET samples, assuming that the DETs are in equilibrium with the colloidal suspensions. The deployment time of 48h is longer than the theoretical time required for the largest colloids in the sample (200 nm) to diffuse in water over a distance of 400 µm, which is the thickness of the DET hydrogel.

The diffusion coefficient D of a 200 nm sized particle in water based on Stokes-Einstein equation:

$$D = \frac{k_B T}{3\pi\eta d} = 2.14 * 10^{-12}\ m^2 s^{-1} \quad \text{(Eqn. 1)}$$

With kB the Boltzmann constant (1.38*10^-23 j/K), T the temperature in K, η the viscosity of water at 20°C (1.002 *10^-3 Pa.s) and d the colloid diameter (m).

The time for a 200 nm-size colloid to diffuse a distance 400 µm in water is about 21 h:

$$t = \frac{L^2}{D} = 74703\ s \quad \text{(Eqn. 2)}$$

With L the distance (m) and D diffusion coefficient in water (m²/s).

This is a lower estimate of DET equilibration time (Harper et al. 1997) because the diffusion coefficients of colloids through hydrogels is lower than in water (Zhang et al. 1999).

The 2-point calibration curve of mass loading on DET (µg/cm²) versus counts is used to calculate mass loading on the BL from measured counts. The mass loadings on the BL of Si, Al, Fe are given in Table S6).

Table S15 Estimated Si, Al, Fe mass loadings on the DET and DGT BL deployed in the suspension of isolated clay and the soil extract.

	Colloid suspension	Si nmol/cm²	Al nmol/cm²	Fe nmol/cm²
DET	Clay	1.4	0.8	0.2
	Soil Extract	22.2	11.8	4.1
DGT	Clay	19.5	7.7	1.9
	Soil Extract	119	48	13

Second, an estimation of truly dissolved Al on the BL was calculated. The Equation calculated the mass per unit area (M/A) of truly dissolved Al on the BL with diffusion through the thin membrane and an assumed diffusive boundary layer of 200 µm, which is typical for mixed solutions (Davison & Zhang, 2016) (Eqn. 3).

$$\frac{M}{A} = \frac{Ct}{\left(\frac{\partial_m}{D_m} + \frac{\partial_{DBL}}{D_w}\right)} \quad \text{(Eqn. 3)}$$

With C (mg/L) the truly dissolved Al concentration in solution (from dialysis, Table S13), t the deployment time (s), δ_m the membrane thickness, D_m the diffusion coefficient through the membrane calculated as the diffusion coefficient in water corrected for the membrane porosity, δ_{DBL} the diffusive boundary layer thickness and D_w the Al diffusion coefficient in water at 20°C.

The estimated amount of truly dissolved Al on the BL based on the dialysis data using Eqn.3 for the clay suspension is 1.56 nmol/cm² and for the soil solution 30 nmol/cm². The Al on the BL deployed in the isolated clay suspension was primarily colloidal, with a total of 6.1 nmol Al/cm² (7.7 – 1.56 nmol Al/cm²), which is an eightfold increase compared to DET, which contained 0.796 nmol colloidal Al/cm² (0.8 – 0.004) . For the soil suspension, the colloidal Al concentration 18.8 nmol Al/cm² (48.5-29.7) was approximately twofold greater compared to DET of 11.7 nmol Al/cm² (11.8-0.08).

The estimation is confirmed by Fe data measured with digestion (not calculated for Al due to the low recovery, Figure S2). The nano-DGT accumulated after 48h 4.38 ± 1.53 nmol Fe/cm², while the DGT accumulated 8.88 ± 2.14 nmol/cm². Therefore, the concentration of colloidal Fe on the DGT BL was calculated as 4.5 nmol Fe/cm² (8.88 – 4.38), neglecting that there is a slight increase in diffusive layer thickness for the nano-DGT due to the dialysis membrane.

References

Zhang, H., Davison, W., 1999. Diffusional characteristics of hydrogels used in DGT and DET techniques.Analytica Chimica Acta 398 (1999) 329–340

Harper, M.P., Davison, W., Tych, W., 1997. Temporal, Spatial, and Resolution Constraints for in Situ Sampling Devices Using Diffusional Equilibration: Dialysis and DE. Environ. Sci. Technol. 31, 3110-3119

Panagos, P., Van Liedekerke, M., Borrelli, P., Köninger, J., Ballabio, C., Orgiazzi, A., Lugato, E., Liakos, L., Hervas, J., Jones, A. Montanarella, L. 2022. European Soil Data Centre 2.0: Soil data and knowledge in support of the EU policies. European Journal of Soil Science, 73(6), e13315. DOI: 10.1111/ejss.13315

Panther, J., Bennet, W.B., Teasdale, P.R., Welsh, D.T., Zhao, H. (2012). DGT Measurement of Dissolved Aluminum Species in Waters: Comparing Chelex-100 and Titanium Dioxide-Based Adsorbent. *Environ. Sci. Technol.* 46, 4, 2267–2275

Guan, D., Wei, T., Yu,G., Luo, J., Li, G. (2024). Technical development for *in situ* measurement of labile silicate in waters and soils. Environmental Technology & Innovation, 34, 103613

Davison W, Zhang H. Diffusion Layer Properties. In: Davison W, ed. *Diffusive Gradients in Thin-Films for Environmental Measurements*. Cambridge Environmental Chemistry Series. Cambridge University Press; 2016:32-65.